Astronomy & Astrophysics

LETTER TO THE EDITOR

Hier ist wahrhaftig ein Loch im Himmel[⋆],[⋆⋆],[⋆⋆⋆]

The NGC 1999 dark globule is not a globule

T. Stanke[1], A. M. Stutz[2,3], J. J. Tobin[4], B. Ali[5], S. T. Megeath[6], O. Krause[2], H. Linz[2], L. Allen[7], E. Bergin[4], N. Calvet[4], J. Di Francesco[8,9], W. J. Fischer[6], E. Furlan[10], L. Hartmann[4], T. Henning[2], P. Manoj[11], S. Maret[12], J. Muzerolle[13], P. C. Myers[14], D. Neufeld[15], M. Osorio[16], K. Pontoppidan[17], C. A. Poteet[6], D. M. Watson[11], and T. Wilson[1]

[1] ESO, Karl-Schwarzschild-Strasse 2, 85748 Garching bei München, Germany
   e-mail: tstanke@eso.org
[2] Max-Planck-Institut für Astronomie, Königstuhl 17, 69117 Heidelberg, Germany
[3] Department of Astronomy and Steward Observatory, University of Arizona, 933 North Cherry Avenue, Tucson, AZ 85721, USA
[4] Department of Astronomy, University of Michigan, Ann Arbor, MI 48109, USA
[5] NASA *Herschel* Science Center, California Institute of Technology, 770 South Wilson Ave, Pasadena, CA91125, USA
[6] Department of Physics and Astronomy, University of Toledo, 2801 West Bancroft Street, Toledo, OH 43606, USA
[7] National Optical Astronomy Observatory, 950 N. Cherry Ave., Tucson, AZ 85719, USA
[8] Department of Physics and Astronomy, University of Victoria, PO Box 355, STN CSC, Victoria BC, V8W 3P6, Canada
[9] National Research Council Canada, Herzberg Institute of Astrophysics, 5071 West Saanich Road, Victoria BC, V9E 2E7, Canada
[10] JPL, California Institute of Technology, Mail Stop 264767, 4800 Oak Grove Drive, Pasadena, CA 91109, USA
[11] Department of Physics and Astronomy, University of Rochester, Rochester, NY 14627, USA
[12] Laboratoire d'Astrophysique de Grenoble, Université Joseph Fourier, CNRS, UMR 571, BP 53, 38041 Grenoble, France
[13] Space Telescope Science Institute, 3700 San Martin Dr., Baltimore, MD 21218, USA
[14] Harvard-Smithsonian Center for Astrophysics, 60 Garden Street, Cambridge, MA 02138, USA
[15] Department of Physics and Astronomy, Johns Hopkins University, 3400 North Charles Street, Baltimore, MD 21218, USA
[16] Instituto de Astrofisica de Andalucia, CSIC, Camino Bajo de Huetor 50, 18008, Granada, Spain
[17] Division of Geological and Planetary Sciences 150-21, California Institute of Technology, Pasadena, CA 91125, USA

ABSTRACT

The NGC 1999 reflection nebula features a dark patch with a size of ∼10 000 AU, which has been interpreted as a small, dense foreground globule and possible site of imminent star formation. We present *Herschel* PACS far-infrared 70 and 160 μm maps, which reveal a flux deficit at the location of the globule. We estimate the globule mass needed to produce such an absorption feature to be a few tenths to a few $M_\odot$. Inspired by this *Herschel* observation, we obtained APEX LABOCA and SABOCA submillimeter continuum maps, and Magellan PANIC near-infrared images of the region. We do not detect a submillimer source at the location of the *Herschel* flux decrement; furthermore our observations place an upper limit on the mass of the globule of ∼2.4 × 10^{-2} $M_\odot$. Indeed, the submillimeter maps appear to show a flux depression as well. Furthermore, the near–infrared images detect faint background stars that are less affected by extinction inside the dark patch than in its surroundings. We suggest that the dark patch is in fact a hole or cavity in the material producing the NGC 1999 reflection nebula, excavated by protostellar jets from the V 380 Ori multiple system.

Key words. ISM: clouds – ISM: individual objects: NGC 1999 – ISM: jets and outflows – infrared: ISM – dust, extinction

1. Introduction

In the year 1774 C.E. Friedrich Wilhelm Herschel first noticed patches of sky in the constellation Scorpio that were devoid of stars. Unable to find even the faintest star in these regions, his sister Caroline reported him to exclaim: "Hier ist wahrhaftig ein Loch im Himmel!" ("Truly there is a hole in the sky here!"). These dark areas are now known to be due to obscuring material (e.g., Barnard et al. 1927): clouds of molecular gas, whose dust content absorbs the light of background stars. Dark clouds, ranging in mass and size from giant molecular clouds (GMCs) to tiny globules, are the sites of star formation in our Galaxy.

NGC 1999 is a small reflection nebula in the LDN 1641 portion of the Orion A GMC, located in a small group of 22 pre-main sequence stars and protostars, including the driving source of the prototypical Herbig-Haro objects HH 1 and HH 2 (Megeath et al., in prep.). It is illuminated by the Herbig Ae/Be star V 380 Ori, a multiple system with a circumsystem disk where the primary is a 100 $L_\odot$ B9 star exhibiting strong emission
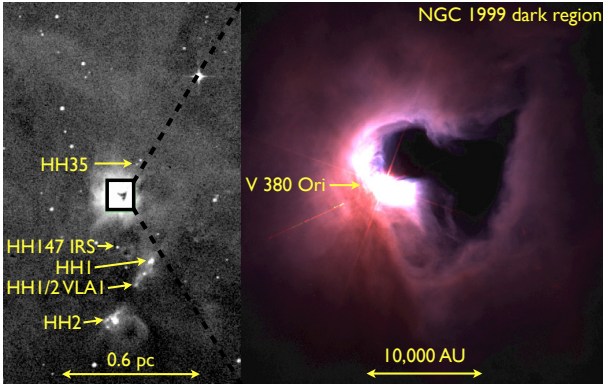
Fig. 1. NGC 1999 and HH 1/2 region (DSS, left) and HST F450W/F555W/F675W true color image of the NGC 1999 dark patch.
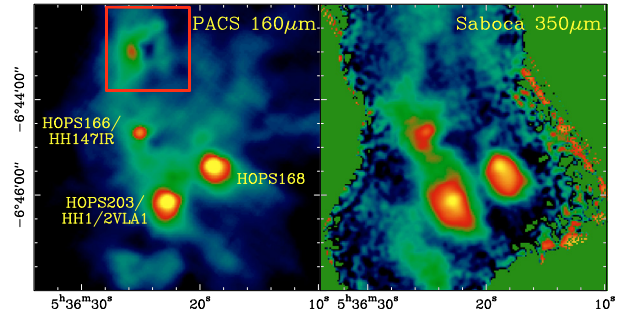

Fig. 2. NGC 1999/HH 1/2 region as seen with *Herschel* PACS at 160 μm (left, the box marks the region shown in Fig. 3), and APEX SABOCA at 350 μm (right, smoothed to 10″ resolution), all displayed with a logarithmic color stretch.

lines (e.g., Leinert et al. 1997; Hillenbrand et al. 1992; Alecian et al. 2009). NGC 1999 features a compact (20–30″) dark patch (see Fig. 1), which is described in the literature as a dark globule and potential site of star formation (e.g., Herbig 1946, 1960; Warren-Smith et al. 1980), but which has never been studied in greater detail before.

We report here the serendipitous and surprising detection with PACS of a 70 and 160 μm flux decrement at the location of NGC 1999. The maps show a dark patch against the nebulous far-IR emission that closely resembles the dark patch seen at visible wavelengths. The MSX, ISO, and *Spitzer* space telescopes have detected clouds in absorption at mid-IR (5–30 μm) wavelengths against the diffuse IR background of the Galaxy (e.g., Bacmann et al. 2000; Stutz et al. 2008; Tobin et al. 2010; Stutz et al. 2009a), in a few cases even at 70 μm (Stutz et al. 2009b). However, the detection of the NGC 1999 globule by PACS would be the first detection of a dark globule in absorption at 160 μm. At wavelengths $\geq$160 μm, cold globules are normally detected through the emission from cold (10–30 K) dust. Furthermore, absorption at these wavelengths requires extinctions in excess of 100 A_V.

Motivated by the possible discovery of a 160 μm dark cloud, we obtained follow-up ground based submillimeter and near-IR (extinction) observations towards the globule. We did not detect the column density or mass of cold dust necessary to produce such an absorption feature in the far-IR. We therefore conclude that the dark globule is actually a cavity in the NGC 1999 cloud carved by outflows from the V 380 Ori system. Thus, the *Herschel* telescope has discovered what truly is a hole in the sky.

2. Observations and processing

2.1. Herschel PACS observations

NGC 1999 was observed with *Herschel* (Pilbratt et al. 2010) with the PACS instrument (Poglitsch et al. 2010) at 70 and 160 μm on 2009 October 9 (OBSIDs 1342185551 and 1342185552) as part of the science demonstration phase observations of the *Herschel* Orion Protostar Survey (HOPS; P.I. S. T. Megeath). The data are presented in Figs. 2 and 3 (see also Fischer et al. 2010). They were processed with the *Herschel* common software system (HCSS[1]) version 3.0 build 919, following standard steps, using v. 4 of the calibration file. After initial processing the two orthogonal scans were combined into a single observation. We

used the same HCSS software modules as the automatic PACS pipeline. We used two different approaches for combining the data into final mosaics:

Method 1: Simple ("naive") mapping with baseline removal. To preserve the extended emission we estimated the sky and the correlated signal drifts observed in PACS readouts (Sauvage et al. 2010). To determine the baselines, we removed pixel-to-pixel electronic offsets using the median of the entire time stream, then calculated the median for each frame/readout. The median values were divided into 500 readout bins, and we took the minimum value for each bin. This approach preserves the extended emission at all spatial scales, but does not remove $1/f$ noise. The final mosaic was created using the "photProject" routine.

Method 2: Optimal mapping with MADmap[2] to remove the bolometer $1/f$ noise from the pixel time-line. The initial processing is the same as for Method 1. However, instead of 'photProject', MADmap is used to determine an optimal solution for each sky pixel. This method preserves extended emission *and* removes the $1/f$ noise, at the price of a reduced sensitivity.

2.2. Other data

APEX SABOCA and LABOCA – We obtained submillimeter continuum maps using LABOCA and SABOCA on APEX. LABOCA (Siringo et al. 2009) is a ~250 bolometer array operating at 870 μm, with a spatial resolution of 19″. Observations were done on 2009 November 29 and 30 in fair conditions, with precipitable water vapour (PWV) values around 1 mm ($\tau_{\mathrm{zenith},870} \sim 0.26$). We used a combination of spiral and straight on-the-fly scans in order to recover extended emission. Data reduction was done with the BOA software (Schuller et al., in prep.) following standard procedures, including iterative source modeling. SABOCA (Siringo et al. 2010) is a 37 bolometer array operating at 350 μm, with a resolution of 7.″8. Data were taken on 2009 December 1st and 3rd (NGC 1999) and on 2008 October 7 and 8 (HH 1/2 area) with PWV < 0.5 mm ($\tau_{\mathrm{zenith},350} < 1$). The observing and data reduction procedures were similar to those used for LABOCA. The 350 μm map is presented in Fig. 2, and both maps in Fig. A.1 (available in electronic form only).

Magellan PANIC – NGC 1999 was observed with the PANIC near-IR camera (2′ field of view) at Magellan on 2009 December 4 in photometric conditions through H, K_s and H_2 filters in 0.″3 to 0.″4 seeing. Separate sky exposures were taken for each filter. The data were reduced with standard near-IR routines in the IRAF UPSQIID package. The photometry is presented in Appendix B. The K_s and H_2 images are shown in Figs. 3 and 4, respectively.

---

[2] Microwave Anisotropy Dataset mapper (Cantalupo et al. 2010, see Poglitsch et al. 2010, for its implementation in HCSS).
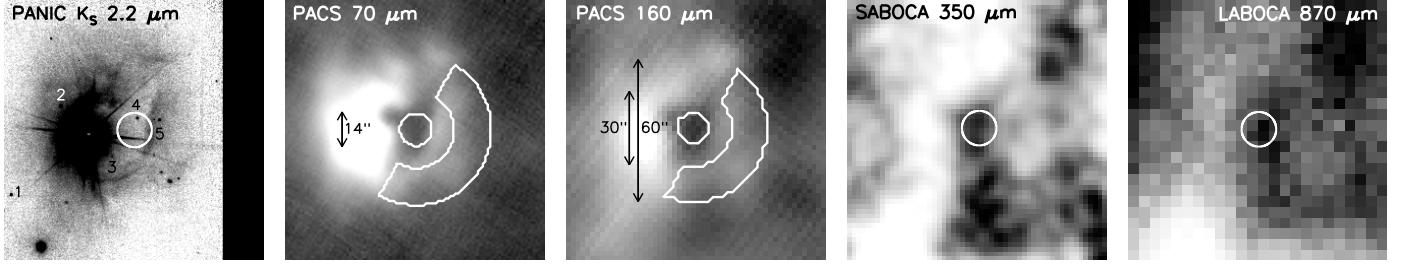
Fig. 3. 1′.75×1′.75 images of the region around NGC 1999 (including V 380 Ori) centered on RA = 5^{h}36^{m}24.4^s, Dec = −06°42′56.4″ (J2000). The white circle (14″ diameter) on the PANIC near-IR K_s image indicates the NGC 1999 region; the image is annotated with the source designations for five faint stars in the field as listed in Table B.1, where we give their ($H − K_s$) colors. The PACS 70 μm and 160 μm maps both show NGC 1999 observed as a flux deficit; the overlays represent the pixel masks used for the analysis of the NGC 1999 feature. The *right-most two panels* show the SABOCA and LABOCA maps.

3. Data analysis

3.1. Herschel 70 μm and 160 μm

A cursory inspection of the *Herschel* data (Figs. 2 and 3) immediately reveals a flux decrement in both PACS maps, which closely follows the morphology of the putative dark globule in NGC 1999. Following Stutz et al. (2009b), we determine the column density and mass of the putative globule in the foreground of NGC 1999, assuming that the observed 70 and 160 μm decrement is due to extinction. The optical depth is given by

$$\tau = -1.0 \cdot \ln[(f + f_{BG})/(f_0 + f_{BG})], \qquad (1)$$

where f is the shadow flux level, f_0 is the intrinsic unabsorbed flux level, and f_{BG} is the background contribution to the flux zero–level in the images. We estimate the shadow flux level f as the mean pixel value in a ∼7″ radius region centered on the darkest part of NGC 1999; the unobscured flux level f_0 is estimated as the median pixel value in a half–annulus with inner and outer radii of 15″ and 30″, with a southwest orientation chosen to avoid the bright V 380 Ori flux. The f and f_0 image regions are over-plotted on the PACS maps in Fig. 3. The f_{BG} flux level is not present in the *Herschel* maps because constant flux level pedestals are removed by the data reduction. We estimate the 70 μm BG flux value by interpolating the *IRAS* 60 and 100 μm images; the 160 μm BG flux values were obtained from the *ISO* Serendipity Survey in the near vicinity of NGC 1999. In both cases we take 50% of the total measured flux as our estimate for f_{BG} as we are only interested in the missing flux originating from *behind* NGC 1999, and not the foreground component. While this assumption is crude, the f_{BG} values are low compared to the f and f_0 levels and do not have a large effect on our analysis.

Following Eq. (1), we calculate the mean optical depth per pixel. Table 1 presents the results for the data reduced with both methods (which we find to agree well, indicating that both recover extended emission equally well). From the resulting optical depth we calculate the column density and mass (in a 7″ radius aperture) required to cause this flux-decrement at the two PACS wavelengths; these are presented in Table 1. We use the extreme Ossenkopf & Henning (1994) model dust opacities for grains with thick ice mantles: κ_{70} = 541 cm^{2}g^{-1} and κ_{160} = 55.7 cm^{2}g^{-1}, a gas-to-dust mass-ratio equal to 100, and a distance of 420 pc (e.g., Menten et al. 2007). The resulting column densities and masses for the two wavelength bands are clearly inconsistent. For example, we derive that masses of 0.1 $M_{\odot}$ and 2.5 $M_{\odot}$ are needed to account for the observed flux decrement in the the 70 and 160 μm data, respectively.
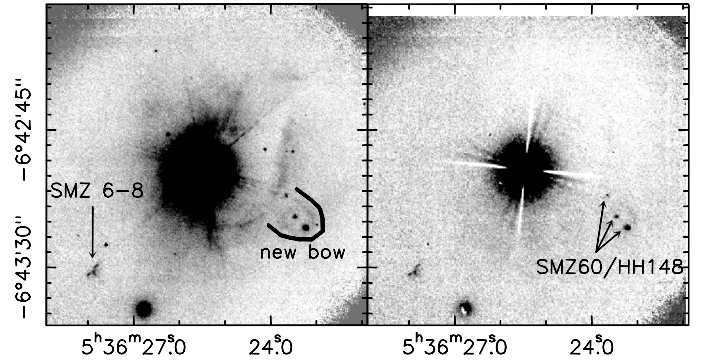

Fig. 4. *Left*: PANIC near-IR H$_2$ narrow-band image of the NGC 1999; *right*: the same image with a scaled K_s continuum image subtracted.

Table 1. Far-infrared optical depth, mass, and column density estimates.

λ μm	$f^{\,a}$ Jy/□″	$f_0^{\,b}$ Jy/□″	$f_{BG}^{\,c}$ Jy/□″	τ	Mass $M_{\odot}$	N(H+He) cm^{-2}
photProject (method 1)
70	0.002	0.003	0.001	0.23	0.1	1.9×10^{22}
160	0.003	0.007	0.002	0.48	2.5	3.8×10^{23}
MADmap (method 2)
70	0.002	0.003	0.001	0.2	0.1	1.6×10^{22}
160	0.004	0.008	0.002	0.45	2.4	3.5×10^{23}

Notes. [a] Derived in a ∼7″ radius region centered on RA = 5^{h}36^{m}24.4^s, Dec = −06°42′56.4″, indicated in Fig. 3 as the inner most circular overlay in the *Herschel* PACS images. [b] Derived in a ∼15″ to ∼30″ radius half-annulus, excluding bright areas associated with V 380 Ori, indicated in Fig. 3 as well. [c] Estimated background flux contribution to the PACS maps, estimated as 50% of the measurements from IRAS data (interpolated to 70 μm) and the 160 μm *ISO* Serendipity Survey near NGC 1999.

3.2. Ground-based follow-up

Neither the APEX 350 nor 870 μm maps show an emission feature at the location of the *Herschel* flux decrement. Instead, the submillimeter emission bears a strong resemblance to the 160 μm emission, suggesting that the 160, 350, and 870 μm maps are all tracing the morphology of the dust emission (Fig. 3). This morphology is suggestive of a diffuse ring of material, not a hot region absorbed by a foreground cold cloud. Assuming optically thin dust emission, total gas+dust masses can be obtained from submillimeter fluxes as

$$M_{G+D} = \frac{M_G}{M_D} \frac{S_\nu d^2}{B_\nu(T_D)\kappa_{\nu,D}}, \qquad (2)$$

where $\frac{M_G}{M_D}$ is the gas-to-dust mass ratio, S_ν the flux density, d the distance, $B_\nu(T_D)$ the Planck function, and $\kappa_{\nu,D}$ the dust opacity.

With an rms noise level of ~13 mJy in our LABOCA map, we should be able to detect (3 σ) a 40 mJy point source, corresponding to a mass of 0.13 $M_\odot$, assuming T_D = 10 K and Ossenkopf & Henning (1994) opacities for thick ice mantle grains. Although the 870 μm sensitivity limits are uncertain due to the surrounding highly structured low surface-brightness emission, we conclude that a mass around 0.1 $M_\odot$ should have been detected in the LABOCA map. More interestingly, the rms noise on the SABOCA map is around 17 mJy, implying a 3σ point-source detection limit of ~50 mJy. Due to the steeply rising Planck function and dust opacity, this limit corresponds to a much lower mass detection limit of only 2.4×10^{-2} $M_\odot$. For comparison, the mass necessary to produce an extinction shadow as derived from the 70 μm map (on the order of 0.1 $M_\odot$) would produce a 350 μm source with a flux of ~200 mJy, i.e., a >10σ detection. This result is in stark contradiction with the dense globule/shadow interpretation of the absorption features observed in the *Herschel* data.

The PANIC images show five faint stars around V 380 Ori, marked in Fig. 3 with their source designation as listed in Table B.1, where we also give their ($H - K_s$) colors and estimated extinction. Stars 3 and 4 are within the dark patch and have moderately red colors, implying a mean extinction of $A_V \sim 10$. In comparison, stars 1, 2, and 5 outside the dark patch are slightly redder and have a mean extinction of $A_V \sim 12$. None of the five stars are apparent in the HST images, indicating that they are background stars (Fig. 1). The $H - K_s$ colors show that the extinction toward the dark patch is much less than the 100 A_V needed to attenuate the 160 μm emission and that the extinction through the dark patch is slightly less than that through the surrounding region.

4. Discussion

Optical images of NGC 1999 show a dark patch suggestive of a small, dense globule obscuring the NGC 1999 reflection nebula. Surprisingly, our 70 and 160 μm images clearly show a dark patch against the bright nebula with a strikingly similar morphology to that in visible light images. These *Herschel* measurements, combined with subsequent ground based data, lead to the conclusion that the dark feature is a hole in the NGC 1999 nebula. First, we find that the masses needed to cause the 70 and 160 μm dark patch – 0.1 and 2.5 $M_\odot$, respectively – are inconsistent. Furthermore, the globule is not detected in emission at 350 and 870 μm: the SABOCA obervations place an upper limit of 2.4×10^{-2} $M_\odot$ for a temperature of 10 K. This upper limit is far below the amount of mass needed to cause the obscuration in the PACS data. Finally, near-IR observations with PANIC detect background stars toward the dark patch; the $H - K_s$ colors of these stars are slightly bluer than stars detected outside the globule, suggesting a lower extinction toward the dark patch. Furthermore, the extinctions of the background stars are less than that required to absorb the 160 μm flux. Taken together, these observation show that the dark patch is not a globule, but instead a cavity in the nebula.

The presence of a well delineated cavity of the size of ~10 000 AU deserves some attention. With the typical turbulent velocities on the order of a few km s^{-1} in clouds, such a cavity should be filled on timescales of at most a few 10 000 yrs and quickly disappear. The PANIC H$_2$ narrow band data (Fig. 4) deliver important hints about the possible origin and peculiar

shape of the cavity. They reveal a previously unknown, faint H$_2$ bow shock enveloping the SMZ 60/HH 148 compact knots (Stanke et al. 2002; Corcoran & Ray 1995), constituting the clearest evidence so far for a collimated flow running northeast to southwest through the cavity. This flow, which likely originates in the V 380 Ori multiple system, could possibly excavate the southern part of the cavity. SMZ 6-8 in the southeastern corner of the PANIC image resembles a small bow shock in a flow coming from the northwest; together with HH 35, located northwest of V 380 Ori (Fig. 1), it indicates a second, northwest to southeast oriented flow, which could be responsible for digging the northwestern lobe of the cavity.

We note a similar flux depression in the 160 μm *Herschel* image southwest of the protostar HOPS 166, which drives the HH 147 outflow (Corcoran & Ray 1995). Optical images (e.g., Fig. 1) show a circular reflection nebula marking the HH 147 outflow cavity, coinciding with the far-IR flux depression. The NGC 1999 dark patch may therefore only be a somewhat peculiar example of a cavity carved in the ambient medium by an outflow, rendered particularly visible by the illumination and heating of the cavity walls by V 380 Ori. Sensitive far-IR maps taken with *Herschel* may therefore provide a new tool to assess the importance of outflow feedback on cloud cores.

References

Alecian, E., Wade, G. A., Catala, C., et al. 2009, MNRAS, 400, 354
Bacmann, A., André, P., Puget, J., et al. 2000, A&A, 361, 555
Barnard, E. E., Frost, E. B., & Calvert, M. R. 1927, A photographic atlas of selected regions of the Milky way, ed. Barnard, E. E., Frost, E. B., & Calvert, M. R.
Campeggio, L., Strafella, F., Maiolo, B., Elia, D., & Aiello, S. 2007, ApJ, 668, 316
Cantalupo, C. M., Borrill, J. D., Jaffe, A. H., Kisner, T. S., & Stompor, R. 2010, ApJS, 187, 212
Corcoran, D., & Ray, T. P. 1995, A&A, 301, 729
Fischer, W. J., Megeath, S. T., Ali, B., et al. 2010, A&A, 518, L122
Herbig, G. H. 1946, PASP, 58, 163
Herbig, G. H. 1960, ApJS, 4, 337
Hillenbrand, L. A., Strom, S. E., Vrba, F. J., & Keene, J. 1992, ApJ, 397, 613
Indebetouw, R., Mathis, J. S., Babler, B. L., et al. 2005, ApJ, 619, 931
Leinert, C., Richichi, A., & Haas, M. 1997, A&A, 318, 472
Menten, K. M., Reid, M. J., Forbrich, J., & Brunthaler, A. 2007, A&A, 474, 515
Ossenkopf, V. & Henning, T. 1994, A&A, 291, 943
Pilbratt, G. L., et al., 2010, A&A, 518, L1
Poglitsch, A., et al., 2010, A&A, 518, L2
Sauvage, M., et al., 2010, A&A, 518, L64
Siringo, G., Kreysa, E., Kovács, A., et al. 2009, A&A, 497, 945
Siringo, G., Kreysa, E., de Breuck, C., et al. 2010, The Messenger, 139, 20
Stanke, T., McCaughrean, M. J., & Zinnecker, H. 2002, A&A, 392, 239
Stutz, A. M., Rubin, M., Werner, M. W., et al. 2008, ApJ, 687, 389
Stutz, A. M., Rieke, G. H., Bieging, J. H., et al. 2009a, ApJ, 707, 137
Stutz, A. M., Bourke, T. L., Rieke, G. H., et al. 2009b, ApJ, 690, L35
Tobin, J. J., Hartmann, L., Looney, L. W., & Chiang, H. 2010, ApJ, 712, 1010
Warren-Smith, R. F., Scarrott, S. M., King, D. J., et al. 1980, MNRAS, 192, 339
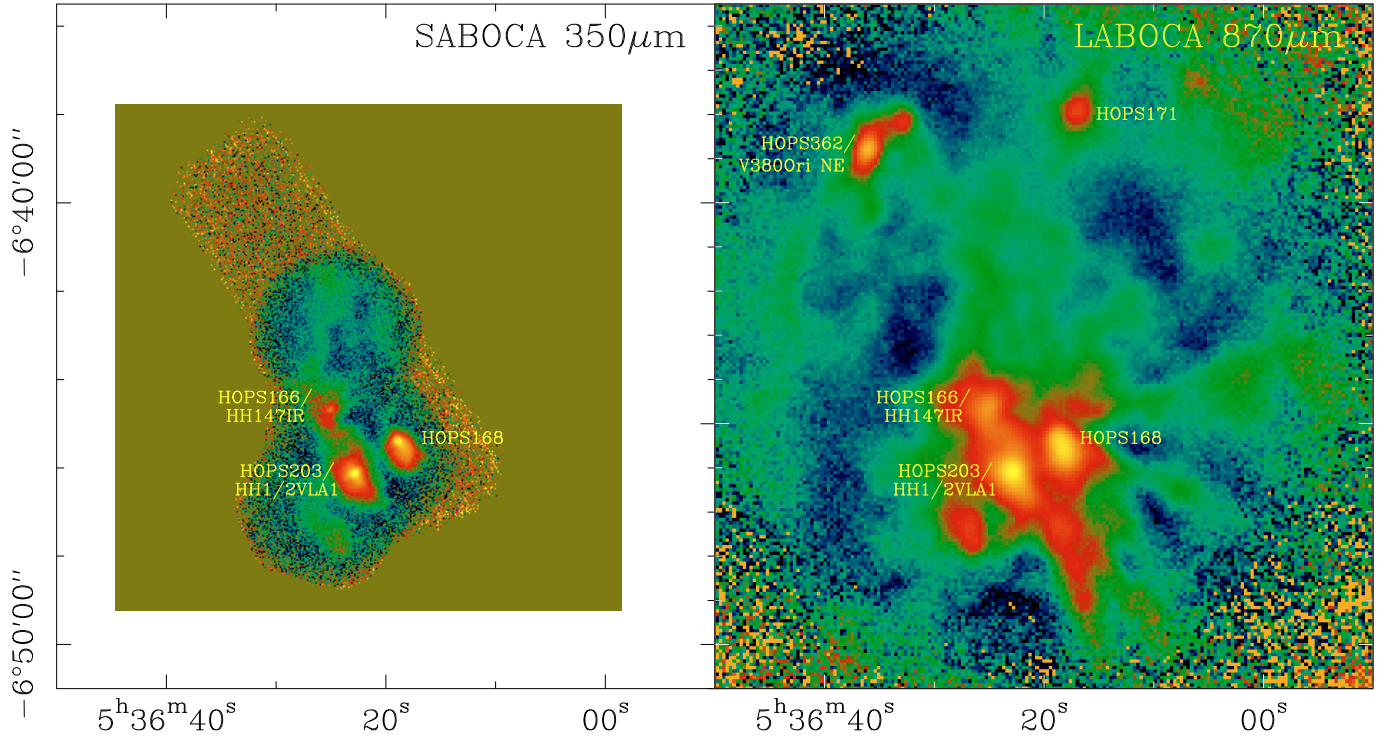
Appendix A: SABOCA and LABOCA submillimeter maps

Fig. A.1. Full submillimeter maps. *Left*: SABOCA, displayed at the original resolution of 7″.8; *right*: LABOCA. Protostars in the field are labeled with their HOPS designations. For both maps a logarithmic color scale is used.

Appendix B: PANIC H and K_s photometry

Table B.1. PANIC NGC 1999 near-IR colors of background stars.

Source [a]	RA (J2000) (h m s)	Dec (J2000) (° ′ ″)	K_S mag	$\sigma(K_S)$ mag	$(H - K_S)$ mag	$\sigma(H - K_S)$ mag
1	05 36 27.54	−06 43 22.29	16.08	0.01	0.83	0.01
2	05 36 26.19	−06 42 46.23	15.68	0.01	0.95	0.02
3	05 36 24.78	−06 43 06.72	18.36	0.10	0.67	0.14
4	05 36 24.09	−06 42 51.12	16.62	0.01	0.84	0.02
5	05 36 23.48	−06 42 51.86	16.71	0.02	0.95	0.02

Notes. [a] See Fig. 3 for source designation.

Five faint stars are visible in the PANIC H and K_s images. Their positions and photometry are listed in Table B.1. Photometric calibration was performed with 2MASS[3] photometry of comparison fields containing 20 2MASS sources and verified with a 2MASS star in the science field. Photometry was conducted with the IRAF task apphot.

The measured $(H - K_S)$ color was used to estimate the extinction A_V toward the stars. We assumed an intrinsic $(H - K_S)$ color of 0.17, derived as the median $(H - K_S)$ colors of stars in an unreddened control field near Orion (Megeath et al., in prep). We adopted the reddening law of Indebetouw et al. (2005) to convert $(H - K_S)$ excess into K-band extinction A_K, from which we obtained the optical extinction as $A_V = 8 \times A_K$, corresponding to a total to selective extinction R_V between the diffuse ISM value of 3.1 and the higher values (up to 5) found for dense clouds (e.g. Campeggio et al. 2007).

---

[3] The Two Micron All Sky Survey is a joint project of the University of Massachusetts and the Infrared Processing and Analysis Center/California Institute of Technology, funded by the National Aeronautics and Space Administration and the National Science Foundation.